Chaos
An Interdisciplinary Journal
of Nonlinear Science

AIP Publishing

Comparison of discretization strategies for the model-free information-theoretic assessment of short-term physiological interactions

Chiara Barà,[1] Laura Sparacino,[1] Riccardo Pernice,[1] Yuri Antonacci,[1] Alberto Porta,[2,3] Dimitris Kugiumtzis,[4] and Luca Faes[1]

[1)]*Department of Engineering, University of Palermo, Viale delle Scienze, Building 9, 90128 Palermo, Italy*

[2)]*Department of Biomedical Sciences for Health, University of Milan, 20133 Milan, Italy*

[3)]*Department of Cardiothoracic, Vascular Anesthesia and Intensive Care, IRCCS Policlinico San Donato, 20097 San Donato Milanese, Milan, Italy*

[4)]*Department of Electrical and Computer Engineering, Aristotle University of Thessaloniki, 54124 Thessaloniki, Greece*

(*Electronic mail: luca.faes@unipa.it)

(Dated: 13 February 2023)

This work presents a comparison between different approaches for the model-free estimation of information-theoretic measures of the dynamic coupling between short realizations of random processes. The measures considered are the Mutual Information Rate (MIR) between two random processes X and Y and the terms of its decomposition evidencing either the individual entropy rates of X and Y and their joint entropy rate, or the transfer entropies from X to Y and from Y to X and the instantaneous information shared by X and Y. All measures are estimated through discretization of the random variables forming the processes, performed either via uniform quantization (binning approach) or rank ordering (permutation approach). The binning and permutation approaches are compared on simulations of two coupled non-identical Hènon systems and on three datasets including short realizations of cardiorespiratory (CR, heart period and respiration flow), cardiovascular (CV, heart period and systolic arterial pressure) and cerebrovascular (CB, mean arterial pressure and cerebral blood flow velocity) measured in different physiological conditions, i.e., spontaneous vs. paced breathing or supine vs. upright positions. Our results show that, with careful selection of the estimation parameters (i.e., embedding dimension and number of quantization levels for the binning approach), meaningful patterns of the MIR and of its components can be achieved in the analyzed systems. On physiological time series, we found that paced breathing at slow breathing rates induces less complex and more coupled CR dynamics, while postural stress leads to an unbalancing of CV interactions with prevalent baroreflex coupling and to less complex pressure dynamics with preserved CB interactions. These results are better highlighted by the permutation approach, thanks to its more parsimonious representation of the discretized dynamic patterns, which allows to explore interactions with longer memory while limiting the curse of dimensionality.

Model-free tools for the analysis of bivariate time series are fundamental to provide a proper description of how the coupling among systems arises from the underlying possibly non-linear regulatory mechanisms. Among the tools devised to perform this analysis, information-theoretic measures are largely explored to infer short-term interactions from pairs of physiological time series. In this context, the so-called mutual information rate (MIR) is a long-known measure of the dynamic interaction between two random processes, which can be reliably approximated from bivariate linear models fitting the observed time series, but is much harder to quantify directly if the model assumptions are not satisfied. In this work, the challenge of performing model-free estimation of this measure is faced exploiting the possibility to decompose the MIR into terms evidencing measures of entropy rate and conditional mutual information, executing low-dimensional time series embedding, and implementing the estimation of these terms through binning- and permutation-based discretization strategies. While the application to short-term simulated and physiological series provides plausible results, it also evidences troublesome aspects that call for the development of improved entropy estimators and refined embedding strategies.

I. INTRODUCTION

In recent years, a wide range of approaches have been proposed to assess the temporal statistical structure and the interaction between coupled dynamic processes from the analysis of bivariate time series taken as realizations of these processes. The most prominent methods are based on state space interdependence[1–3], correlation analyses[4,5], or on the concept of Granger causality (GC) implemented in the time or frequency domains[6,7]. A general and flexible framework, which encompasses most of these approaches, is the framework of information dynamics[8], which has been developed and widely exploited to characterize the interdependence of coupled systems in several fields including neuroscience[9] and physiology[10,11]. In particular, entropy-based measures quantifying the dynamical complexity or information storage within a single process[12,13], or the directed information transfer from one process to another[14,15], have been successfully used to assess physiological interactions in the cardiorespiratory[10], cardiovascular[16] and cerebrovascular[17] systems.

A long-known and well-defined measure to assess the dy-

namic coupling between two time series using information theory is the Mutual Information Rate (MIR), which quantifies the information exchanged over time by two coupled systems[18,19]. However, since the MIR is defined for infinite-dimensional variables, its reliable estimation in practical contexts where short stationary realizations are typically available is a daunting task. In spite of this, a renewed interest for this measure has recently emerged thanks to the possibility to decompose it in different forms evidencing measures of entropy rate or conditional mutual information[20], and thanks to the development of accurate estimators for the constituent terms[21–24]. The interest in this approach stems also from the fact that the terms appearing in the decomposition of the MIR constitute popular measures such as the conditional entropy[25] or the transfer entropy[14]; these measures are related respectively to the concepts of complexity and causality, whose computation is relevant *per se* in several applications. Nevertheless, the analysis of the MIR and its constituent terms has been faced up to now for specific classes of coupled random processes, such as continuous-time point processes[22] or discrete-time linear Gaussian processes[26]. The estimation of these measures in the more general case where assumptions about the type of processes or about the form of interactions to be analyzed are relaxed remains a challenging task that has received less attention up to now.

The present work faces the problem of estimating the MIR and the terms of its decomposition using model-free entropy estimates. Model-free approaches are alternative to parametric estimators, which have the advantage of favoring computation but the drawback of losing generality. Indeed, regardless of whether linear[27] or nonlinear[6] model-based methods are used, constraining the analysis on a specific model structure limits the capability to detect and describe complex interactions and multifaceted dynamic behaviors. Here, we employ a model-free strategy for the computation of the information shared dynamically between two random processes, which is described as follows. First we express the MIR equivalently as the sum of the individual entropy rates of each process minus their joint entropy rate, or as the sum of the transfer entropy computed along the two directions of interaction plus the instantaneous information shared by the processes at zero lag. Second, to allow computation of the measures from finite-length realizations of the processes, we perform low-dimensional embedding approximating the past histories of the processes with a small number of time-lagged components. Third, among the variety of methods for the nonparametric estimation of dynamic information measures[28], we employ discretization methods, which compute the relevant entropy terms on discrete random variables obtained through symbolization of the observed continuous-valued vector variables. Specifically, the approaches to discretization used herein are: (i) the binning method performing uniform quantization of the time series samples[29]; and (ii) the permutation method working on the ranks of the amplitude values within patterns extracted from the time series[30].

The binning- and permutation-based discretization approaches are first compared in simulations of two coupled nonlinear Hènon systems. Then, they are applied to three datasets of physiological time series collected from young healthy subjects and including different pairs of series measured in three experimental protocols: (i) heart period and respiratory flow measured during spontaneous and paced breathing; (ii) heart period and systolic arterial pressure measured at rest and during head-up tilt; and (iii) mean arterial pressure and cerebral blood flow velocity measured at rest and during head-up tilt. These applications have been chosen because they feature challenging conditions where complex short-term physiological mechanisms need to be inferred using model-free methods applied on short realizations ($\sim$ 250-300 points). In this context, the comparison between the two discretization approaches is made observing their ability to reveal expected physiological responses while facing two contrasting needs, i.e., working in low-dimensional spaces and providing an accurate description of the process dynamics in terms of time-lagged interactions and signal amplitude.

II. METHODS

Let us consider two possibly interacting dynamical systems $\mathscr{X}$ and $\mathscr{Y}$, and assume that their joint evolution over time is described by the stochastic processes $X = \{X_n\}$ and $Y = \{Y_n\}$, where n is the time counter. To introduce the notation, let us indicate as X_n, Y_n the scalar random variables describing the current state of X and Y, as $X_{n-k:n-1} = [X_{n-k} \cdots X_{n-1}]$ and $Y_{n-k:n-1} = [Y_{n-k} \cdots Y_{n-1}]$ the k-dimensional vector variables sampling X and Y over the past k lags, and as $X_{<n} = \lim_{k\to\infty}(X_{n-k:n-1})$ and $Y_{<n} = \lim_{k\to\infty}(Y_{n-k:n-1})$ the infinite-dimensional variables sampling X and Y over their whole past history. In this work we consider the problem of estimating the dynamic coupling between the two systems through the so-called Mutual Information Rate (MIR)[18]. In the following subsections we will first provide the theoretical formulation of the MIR and of its information-theoretic decomposition, and then illustrate the binning and permutation approaches for the estimation of the MIR and its terms starting from two scalar time series $\boldsymbol{x} = \{x_n\}_{n=1}^N$ and $\boldsymbol{y} = \{y_n\}_{n=1}^N$, observed as realizations of the processes X and Y under analysis.

A. Mutual Information Rate Decomposition

The MIR between two stationary and ergodic stochastic processes X and Y is defined as

$$I_{X;Y} = \lim_{k\to\infty} \frac{1}{k} I(X_{n-k:n-1}; Y_{n-k:n-1}), \tag{1}$$

where $I(\cdot;\cdot)$ is the mutual information between two random variables. The MIR is a dynamic measure of the information exchanged per unit of time between two dynamical systems[18], which has been implemented in different forms to quantify dynamic interactions between physiological processes[21,22,24]. The popularity of this measure stems also from the fact that it can be decomposed evidencing information quantities that have meaningful interpretation and are practically computable

from time series data. In fact, starting from the equivalent definitions of entropy rate of an ergodic stochastic process X[31]:

$$H_X = \lim_{k\to\infty} \frac{1}{k} H(X_{n-k:n-1}) = H(X_n|X_{<n}), \tag{2}$$

where $H(\cdot)$ denotes entropy and $H(\cdot|\cdot)$ denotes conditional entropy, some elaborations (see, e.g., the supplemental material of Mijatovic et al.[22]) lead to the expansions:

$$I_{X;Y} = H_X + H_Y - H_{X,Y}, \tag{3}$$
$$I_{X;Y} = T_{X\to Y} + T_{Y\to X} + I_{X\cdot Y}. \tag{4}$$

The first decomposition of the MIR given in (3) evidences how it can be formulated comparing the sum of the individual entropy rates of the analyzed processes X and Y, H_X and H_Y, with their joint entropy rate $H_{X,Y}$; the entropy rate is a well-known measure of complexity expressed as the conditional entropy of the present state of a process given its own past history[29,32]. On the other hand, the decomposition (4) expresses the MIR as the sum of the two transfer entropies from X to Y and from Y to X, $T_{X\to Y}$ and $T_{Y\to X}$, plus a term quantifying the instantaneous information shared by X and Y at zero lag, $I_{X\cdot Y}$; the transfer entropy (TE) is a very popular measure of directed information transfer related to the concept of Granger causality[14], while the instantaneous transfer is a symmetric measure related to the concept of instantaneous causality[20].

The two decomposition of the MIR are illustrated graphically in Fig. 1 making use of Venn diagrams. This representation helps understanding how all the measures appearing in the decompositions (3) and (4) can be expressed in terms of conditional entropies, i.e.:

$$H_X = H(X_n|X_{<n}); \tag{5a}$$
$$H_Y = H(Y_n|Y_{<n}); \tag{5b}$$
$$H_{X,Y} = H(X_n,Y_n|X_{<n},Y_{<n}); \tag{5c}$$
$$T_{X\to Y} = H(Y_n|Y_{<n}) - H(Y_n|X_{<n},Y_{<n}); \tag{5d}$$
$$T_{Y\to X} = H(X_n|X_{<n}) - H(X_n|X_{<n},Y_{<n}); \tag{5e}$$
$$I_{X\cdot Y} = H(X_n|X_{<n},Y_{<n}) - H(X_n|X_{<n},Y_n,Y_{<n}). \tag{5f}$$

The expressions in (5) constitute the basis for the practical computation of the MIR decompositions adopted in this work. First, under the Markov assumption stated with memory m, the past history of each process is approximated with m-dimensional vector variables, i.e., $X_{<n} \approx X_{n-m:n-1}$ and $Y_{<n} \approx Y_{n-m:n-1}$ (note that $[Y_nY_{<n}]$ in (5f) becomes $Y_{n-m:n}$). Moreover, we exploit the fact that any conditional entropy can be expressed as the difference between two entropy terms: for instance, the approximation of the conditional entropy in (5c) can be written as $H(X_n,Y_n|X_{n-m:n-1},Y_{n-m:n-1}) = H(X_{n-m:n},Y_{n-m:n}) - H(X_{n-m:n-1},Y_{n-m:n-1})$. Therefore, computation amounts to estimate the entropy of the vector variables sampling the present and past states of the processes combined as described above, and then to plug this estimates into (5) and (3,4) to obtain estimates of the MIR and of its terms. In the next subsections we present two symbolization methods for the computation of the MIR decomposition,

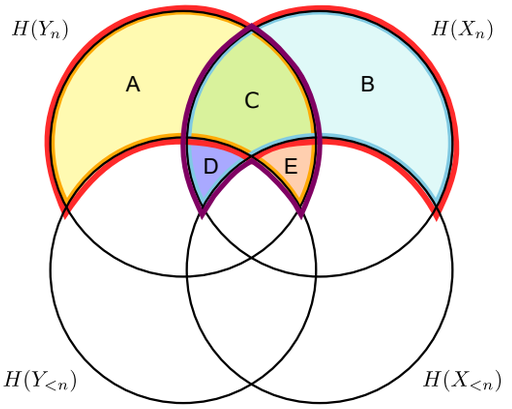

FIG. 1. Venn diagram depicting the MIR decomposition measures defined for two random processes X and Y. Taking the areas of the four circles as the entropy of the present state (upper circles) and of the past history (lower circles) of X (right) and Y (left) one can see that: the entropy rate of X is the union of the portions B, C and D (H_X, Eq. (5a), area with azure contour); the entropy rate of Y is the union of A, C and E (H_Y, Eq. (5b), area with yellow contour); the entropy rate of $\{X,Y\}$ is the union of A, B and C ($H_{X,Y}$, Eq. (5c), area with red contour); the transfer entropy from X to Y is the portion E ($T_{X\to Y}$, Eq. (5d), orange area); the transfer entropy from Y to X is the portion D ($T_{Y\to X}$, Eq. (5e), blue area); and the instantaneous information shared between X and Y is the portion C ($I_{X\cdot Y}$, Eq. (5f), green area). As a result, the MIR between X and Y is the union of C, D and E ($I_{X;Y}$, Eqs. (3,4), area with purple contour).

which estimate the entropy of discrete random variables obtained from the observed continuous variables either using quantization levels or ordinal patterns.

B. Binning approach

The binning method is probably the most intuitive approach to estimate entropy measures for continuous random variables via symbolization[28,29]. This approach is based (i) on building discrete random variables through quantization of the continuous-valued variables, and (ii) computing entropies from the probabilities estimated for the discrete variables via the frequentistic approach. For a generic random variable V taking values in the continuous domain $\mathscr{D}_V = [v_{\min}, v_{\max}]$, quantization returns a discrete random variable B_V taking values in the alphabet $\mathscr{A}_{B_V} = \{1,\ldots,b\}$ formed by b quantization levels, or bins; in the case of uniform quantization, the discretization rule is that an observation of V, $v \in \mathscr{D}_V$, is transformed in the observation of B_V, $b_v = i$, if $v_{\min} + (i-1)r \le v < v_{\min} + ir$, where $r = (v_{\max} - v_{\min})/b$ is the bin amplitude. Once binning is performed, the probability of each discrete value in $\mathscr{A}_{B_V}$ is estimated naturally as the frequency of occurrence of the value over many observations, and an estimate of the entropy of V is the entropy of B_V obtained by the classical formula

$$\hat{H}(V) = -\sum_{b_v\in\mathscr{A}_{B_V}} \hat{p}(b_v)\log\hat{p}(b_v). \tag{6}$$

The formulations above hold intuitively also for vector variables, for which quantization is applied over each scalar component; in the case of an original d-dimensional continuous variable $\mathbf{V} = [V_1 \cdots V_d]$, which is quantized using b bins for each dimension, the corresponding discrete vector random variable $B_{\mathbf{V}} = [b_{V_1} \cdots b_{V_d}]$ takes values inside an alphabet formed by b^d symbols.

In the case of two random processes X and Y relevant for this work, the vector random variables whose entropies are needed to compute the measures listed in (5) are formed combining the present state and the histories sampled up to m past lags of the two processes. For instance, the binning estimator of the conditional entropy term H_X in (5a) works with the m-dimensional variable $X_{n-m:n-1}$ sampling the past of X and with the $(m+1)$-dimensional variable $X_{n-m:n} = [X_{n-m:n-1} X_n]$ sampling the present and the past of X. Starting from the time series $\boldsymbol{x} = \{x_n\}_{n=1}^{N}$, $N-m$ observations of $X_{n-m:n-1}$ and $X_{n-m:n}$ are obtained which take, after quantization, values inside alphabets composed by b^m and b^{m+1} symbols, respectively. Then, after estimating the probability of occurrence of each observation, the entropies $\hat{H}(X_{n-m:n-1})$ and $\hat{H}(X_{n-m:n})$ are estimated using (6), and the entropy rate is computed as $\hat{H}_X = \hat{H}(X_{n-m:n}) - \hat{H}(X_{n-m:n-1})$. The same formulation can be applied for estimating the entropy rate H_Y starting from the time series $\boldsymbol{y} = \{y_n\}_{n=1}^{N}$, while the joint vector variables $[X_{n-m:n-1} Y_{n-m:n-1}]$ and $[X_{n-m:n} Y_{n-m:n}]$ are needed to compute the joint entropy rate (5c); in the latter case, the discrete variables visit spaces of dimension b^{2m} and b^{2m+2}, and need to be estimated from $N-m$ observations. The computation of the TE and instantaneous information sharing in Eqs. (5d,e,f) is even more intricate since it requires the computation of four entropy terms, as each of the two conditional entropy terms is defined as the difference of entropy terms according to the rule $H(V|W) = H(V,W) - H(W)$ holding for any two variables V and W. In the case of the TE, the four entropy terms involve: the vector variables sampling the past history of the target process taken alone (dimension b^m), or taken together with the present state of the same process (dimension b^{m+1}); and the past of both processes taken alone or together with the present of the target (dimensions b^{2m}, b^{2m+1}); in the case of the instantaneous information shared by the two processes, they involve the history of both processes taken alone (dimension b^{2m}), with the present of one of the two processes (dimension b^{2m+1}), or with the present of both processes (dimension b^{2m+2}).

C. Permutation-based approach

The approaches based on permutations perform symbolization working directly on vector variables, taking into account the amplitude order of neighboring samples within the realizations of these variables without effective consideration of their absolute amplitude values[30]. For a generic d-dimensional continuous random variable $\mathbf{V} = [V_1 \cdots V_d]$, realizations of the associated discrete variable $R_{\mathbf{V}}$ are obtained through a rank ordering procedure as follows: if $\mathbf{v} = [v_1 \cdots v_d]$ is a realization of $\mathbf{V}$, the corresponding realization of $R_{\mathbf{V}}$ is $r_{\mathbf{v}} = [r_{v_1} \cdots r_{v_d}] \in \mathscr{A}_{R_{\mathbf{V}}}$, where $r_{v_i} \in \{1, \ldots, d\}$ is the rank order of v_i inside the sequence $\mathbf{v}$ rearranged in ascending order (e.g., $r_{v_i} = 1$ if $v_i = \min(\mathbf{v})$ and $r_{v_i} = d$ if $v_i = \max(\mathbf{v})$; for two equal components of $\mathbf{v}$ the smallest rank is assigned to the component appearing last). Once discretization is performed, the probability of each discrete vector value belonging to the alphbet $\mathscr{A}_{R_{\mathbf{V}}}$ is estimated naturally as the frequency of occurrence of the value over many observations, and an estimate of the entropy of $\mathbf{V}$ is the entropy of $R_{\mathbf{V}}$ obtained as

$$\hat{H}(\mathbf{V}) = -\sum_{r_{\mathbf{v}} \in \mathscr{A}_{R_{\mathbf{V}}}} \hat{p}(r_{\mathbf{v}}) \log \hat{p}(r_{\mathbf{v}}). \tag{7}$$

We note that the discrete random variable $R_{\mathbf{V}}$ obtained applying the permutation strategy to the continuous d-dimensional variable $\mathbf{V}$ takes values inside an alphabet with cardinality $|\mathscr{A}_{R_{\mathbf{V}}}| = d!$, which is usually smaller than the cardinality of the alphabet obtained quantizing the variable with b bins, $|\mathscr{A}_{B_{\mathbf{V}}}| = b^d$. This favors the permutation strategy for the estimation of entropy from a limited number of observations of the variable under analysis.

As for the binning approach, the entropy measures needed to compute the terms of the MIR decomposition in (5) are estimated from observations of the present and past states of the analyzed processes X and Y. Again, the variables $X_{n-m:n}$, $X_{n-m:n-1}$ and $Y_{n-m:n}$, $Y_{n-m:n-1}$ are considered for the estimation of the individual entropy rates $\hat{H}_X$ and $\hat{H}_Y$ in (5a,b), and the joint variables $[X_{n-m:n} Y_{n-m:n}]$ and $[X_{n-m:n-1} Y_{n-m:n-1}]$ are considered to estimate the joint entropy rate $\hat{H}_{X,Y}$ in (5c); the alphabet sizes are $(m+1)!$ and $m!$, and $((m+1)!)^2$ and $(m!)^2$, respectively for the individual and joint entropy rates. As regards the computation of the TE terms in (5d,e), the involved variables are the past history of the target process taken alone or together with its present state (alphabet sizes $m!$ or $(m+1)!$), and the history of both processes taken alone or together with the past of the target (alphabet sizes $(m!)^2$ or $m! \cdot (m+1)!$). Finally, the variables involved in the computation of the instantaneous information sharing are those covering the history of both processes taken alone, taken with the present of one of the two processes, or taken with the present of both processes, which have alphabet size $(m!)^2$, $m! \cdot (m+1)!$, and $((m+1)!)^2$, respectively.

It is worth noting that the approach which we follow to compute any measure of entropy rate is different than that used in several studies working with permutations where the observable corresponding to the present state of a system (e.g., X_n) is converted to a rank vector[33,34]. Our approach is rather similar to that followed in the works of Kugiumtzis[35,36], where such an observable is taken as a scalar and is considered together with the observable of the past m states of the same system (e.g., $X_{n-m:n-1}$) in the formation of the joint state (e.g., $X_{n-m:n}$) from which rank ordering is performed. This approach conforms with the definition of conditional entropy, and has been shown to lead to less biased entropy estimates[35].

D. Practical implementation

1. Parameter setting

A crucial aspect in the implementation of the discretization approaches is the selection of the free parameters for the analysis, i.e., the length of the memory used to cover the past history of the processes (parameter m) and, for the binning estimator, the number of quantization levels used for coarse graining (parameter b). The choice of these parameters is connected to the issue of estimating the entropy of high-dimensional variables from finite-size datasets, which in turn relates to the so-called curse of dimensionality[29,37]. In the practical application of symbolization methods, empirical criteria suggest to optimize the parameters in a way such that the alphabet size remains as low as the length N of the series[29]. In the case of the analysis of the MIR and of its decomposition terms, the most challenging condition occurs in estimating the entropy of the vector variable that covers the past and present states of both processes, i.e., $[X_{n-m:n}Y_{n-m:n}]$; this indeed results in an alphabet size equal to b^{2m+2} in the case of binning and to $((m+1)!)^2$ in the case of the permutation approach.

2. Surrogate data analysis

When applied to finite-length time series, the procedures described above unavoidably return entropy estimates that deviate from the values expected in the cases of full randomness (maximum entropy rate) or full uncoupling (zero information shared or information transfer). Therefore, there is the need to assess the statistical significance of each measure estimated from a given pair of time series. In this work, such an assessment was performed using surrogate data. In particular, since to assess the statistical significance of conditional entropy measures (i.e., H_X, H_Y and $H_{X,Y}$) the whole temporal statistical structure of the series needs to be destroyed, random shuffle surrogates[38] were generated according to the null hypothesis of independent and identically distributed random variables; this was performed by permuting randomly and independently the order of the samples in the two series. On the contrary, to assess the significance of conditional mutual information measures (i.e., $T_{X\to Y}$, $T_{Y\to X}$, and $I_{X;Y}$), as well as of the MIR, it is sufficient to destroy the coupling of the two series, while it is preferable to maintain the statistical properties of the individual series[39]. Therefore, random time shift bivariate surrogates were generated according to the null hypothesis of independent random processes; this was performed by shifting the samples of one of the two time series over time (while wrapping the extra values around the beginning of the series) and leaving the other series unchanged[3].

After generating a set of surrogate time series for each pair of original time series, the considered information measure were computed both on the original series and on the surrogate pairs. Then, a non-parametric test based on percentiles was adopted, distinguishing the two types of measures: each conditional entropy measure was deemed as statistically significant if its value computed on the original series was lower than the 5$^{\text{th}}$ percentile of its distribution derived from the random shuffling surrogates; each conditional mutual information measure was deemed as statistically significant if its value computed on the original series was higher than the 95$^{\text{th}}$ percentile of its distribution derived from the random time shift surrogates.

III. SIMULATION STUDY

In this section we test the estimation approaches proposed in Sect. II for the computation of the dynamic information measures composing the MIR on a chaotic bivariate system. The system considered is a nonlinear deterministic system composed by two coupled non-identical Hènon maps[3,40]; it is defined by the following equations:

$$x_n = 1.4 - x_{n-1}^2 + 0.3x_{n-2} + c_2(x_{n-1}^2 - y_{n-1}^2); \tag{8a}$$
$$y_n = 1.4 - y_{n-1}^2 + 0.1y_{n-2} + c_1(y_{n-1}^2 - x_{n-1}^2), \tag{8b}$$

where the constants c_1 and c_2 determine the strength of coupling in the directions from x to y and from y to x, respectively. In the simulation, the parameter c_2 was fixed to 0.05 to reproduce a weak strength of coupling from y to x, while the parameter $c_1 = c$ was varied from 0 to 0.3 in steps of 0.05. One-hundred realizations of the process were generated for each value of c by varying the initial conditions (equally for the two systems). The length of the analyzed series was set to 300 points to match the short data size of the real application to physiological time series. For each realization, the series to be analyzed were taken after discarding the early transient responses.

A. Data analysis

In the simulation study, binning and permutation approaches were implemented using different combinations of the estimation parameters to emphasize the need to reach a fair compromise between representing accurately the dynamics and limiting the curse of dimensionality. As regards the binning approach, the discretization parameters were fixed to $b = 2$ and $m = 3$, $b = 3$ and $m = 2$, and $b = 4$ and $m = 1$, so as to deal with a maximum number of quantization levels equal to $2^{2\cdot3+2} = 256$, $3^{2\cdot2+2} = 729$, and $4^{2\cdot1+2} = 256$, respectively. We note that, although the first and the last settings adhere to the empirical rule reported in Sect. II D.1, the former binarizes the variables describing the system missing most of the information carried in amplitude, while the latter restricts the observation of the past to the sample immediately preceding the current one, losing a significant part of the dynamic information. On the other hand, the choice $b = 3, m = 2$ appropriately takes into account both the amplitudes and the dynamics of the processes (i.e., $b = 3$ and $m = 2$), but leads to working with considerably more quantization levels than the series length. Regarding the permutation approach, the embedding vector dimension was fixed to $m = 2$, $m = 3$, and $m = 4$, so as to work with ordinal patterns of maximum alphabet size equal to $((2+1)!)^2 = 36$, $((3+1)!)^2 = 576$, and $((4+1)!)^2 = 14400$,

respectively. Although interactions with longer memory are taken into account as m increases, we expect that estimates involving higher dimensional variables may have non-negligible bias.

The statistical significance of each estimated entropy rate and conditional mutual information term, as well as of the global MIR measure, was assessed using surrogate data analysis reported in Sect. II D.2. Specifically, for each pair of simulated time series, 100 surrogates were generated; as regard the implementation of the time shift surrogates, the shift of the time series Y was chosen randomly imposing a minimum shift of 20 lags.

B. Simulation results

Fig. 2 shows the mean and standard deviation of the estimated values of the MIR measure and of its information terms decomposition computed for 100 realizations of the coupled Hènon systems at varying the coupling strength from X to Y, obtained using the binning (a-g) and permutation-based (h-n) approaches . The statistical significance of all estimated measures is reported in Fig. 3.

In general, as the coupling strength from X to Y increases, we observe a rise of the MIR $I_{X;Y}$, which captures the larger exchange of information between the two processes (Figs. 2a,h). This trend is reflected by the TE from X to Y (Figs. 2e,l), while it is not observed for the term $T_{Y\to X}$ (Figs. 2f,m); this behavior is expected, since the dependence of X on Y is unrelated to c (Eq. (8a)). Although these Hènon maps are generated without zero-lag interactions between the two systems, Figs. 2g,n show an increasing trend of the information shared instantaneously; the values of $I_{X\cdot Y}$ become large and significant for large values of c, possibly reflecting the high synchronization of the dynamics when the systems become strongly coupled. Looking at the measures of entropy rate quantifying the complexity of the internal dynamics of the individual processes, we observe that the complexity of Y tends to increase for $c > 0$ (Figs. 2c,j), while the complexity of X is substantially unchanged (Figs. 2b,i). This behavior reflects the fact that the dynamics of Y become more complex as c increases, while those of X are unaffected by variations of c. Looking at the complexity of the joint system, i.e., $H_{X,Y}$, an opposite trend is observed than H_Y (Figs. 2d,k). This behavior may be expected because, as c increases, the dependence of Y both on X and on its own past history increases (Eq. (8b)) (the latter is related to the dependence of X from the past of Y as expressed in Eq. (8a)).

The trends reporting the percentage of significant values of the measures, depicted in Fig. 3, are in agreement with the average values in Fig. 2. In fact, as the coupling parameter c increases, the MIR (Figs. 3a,h), the TE from X to Y (Figs. 3e,l) and the term related to instantaneous interactions (Figs. 3g,n) become progressively more significant, while the entropy rates are always statistically significant (Figs. 3b-d,i-k). In spite of these general trends, differences emerge looking at the different parameter settings. As regards the binning approach, in the case of binarization of the variables (i.e., $b = 2$ and $m = 3$), all measures present lower values than in the other conditions; indeed, the use of only two bins for the discretization of the series amplitude leads to a considerable loss of information, evidenced by the lower number of significant values obtained for $T_{Y\to X}$ and $I_{X\cdot Y}$ compared to the setting $b = 4$ and $m = 1$ (Figs. 3f,g). The same figures also show low significance levels for these measures computed with $b = 3$ and $m = 2$, which may be induced by the use an alphabet size higher than the number of samples of the series. Similarly, permutation-based estimates of measures involving higher-dimensional variables show low significance levels if computed using embedding variables of dimension $m = 4$ (see Figs. 3h,k,l,m,n). On the other hand, we note that the estimates obtained setting $m = 2$, even showing comparable or slightly lower significance than those obtained setting $m = 3$ (except for $I_{X\cdot Y}$ (Fig. 3n)), are not able to fully capture the system dynamics and the change in the coupling strength, leading to an overestimation of the term $H_{X,Y}$ (Fig. 2k) and an underestimation of the MIR (Fig. 2h) and of the terms $T_{X\to Y}$ and $T_{Y\to X}$ (Fig. 2l,m).

IV. APPLICATIONS TO PHYSIOLOGICAL TIME SERIES

This section reports the application of the two strategies presented in Sect. II for the computation of the dynamic information measures composing the MIR to three different types of pairwise interactions typically analyzed in the context of short-term physiological variability. Specifically, the proposed methodology is applied to assess cardiorespiratory interactions during spontaneous and paced breathing (Section IV A.1), as well as cardiovascular or cerebrovascular interactions during rest and postural stress (Sections IV A.2 and IV A.3).

A. Experimental protocols

1. *Cardiorespiratory variability analysis*

Cardiorespiratory interactions were investigated exploiting an historical database collected for the analysis of short-term physiological variability during paced breathing[41] (*database 1*). The database includes physiological time series measured from 19 young healthy subjects monitored in the resting supine position during four experimental conditions: spontaneous breathing (SB), controlled breathing at 10 breaths/minute (C10), at 15 breaths/minute (C15) and at 20 breaths/minute (C20). The first analyzed time series is the sequence of the heart periods (RR intervals) extracted from the electrocardiographic (ECG) signal, given as the time intervals between two consecutive ECG R peaks. The second time series contains the respiratory amplitude values (RESP) extracted from the nasal respiration flow signal sampled at the onset of each heart period (see Fig. 4a). For each subject and condition, synchronous time series of 256 values were considered for the analysis. Further details on the experimental

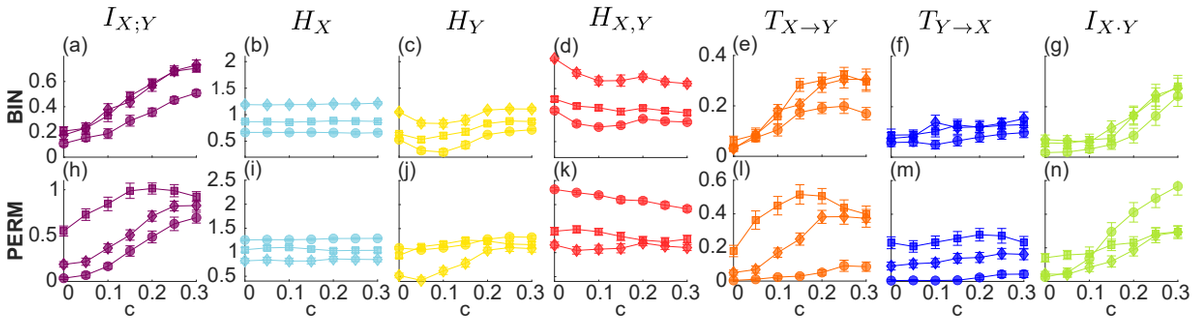

FIG. 2. Estimation of the MIR and its decomposition measures computed on simulations of bidirectionally coupled non-identical Hènon systems with fixed coupling strength from Y to X and coupling strength from X to Y modulated by the parameter c. Panels depict errorbar plots of the MIR ($I_{X;Y}$), of the conditional entropy terms (Eq. (3), H_X, H_Y, $H_{X,Y}$) and of the conditional mutual information terms (Eq. (4), $T_{X\to Y}$, $T_{Y\to X}$, $I_{X\cdot Y}$) computed over 100 simulations using the binning approach (a-g) and the permutation approach (h-n) for discretization. Results are shown at varying the parameter c for different combinations of the discretization parameters: $b = 2$ and $m = 3$ (circles), $b = 3$ and $m = 2$ (squares), and $b = 4$ and $m = 1$ (diamonds) for the binning approach; $m = 2$ (circles), $m = 3$ (diamonds), and $m = 4$ (squares) for the permutation approach.

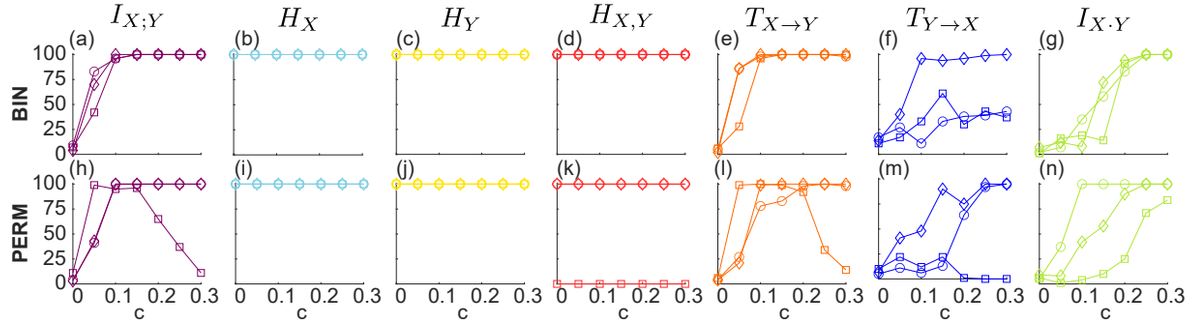

FIG. 3. Results of surrogate data analysis applied on estimates of the MIR and its decomposition measures computed on simulations of bidirectionally coupled non-identical Hènon systems. Plots report the number of realizations, out of 100 simulation runs, for which the measure was detected as statistically significant for each value of the coupling parameter c and for each setting of the discretization parameters. Plots and symbols are the same as in Fig. 2.

protocol, signal acquisition, and time series extraction procedure can be found in the reference paper[41].

2. *Cardiovascular variability analysis*

Cardiovascular interactions were investigated exploiting a historical dataset collected for the study of the short-term physiological response of the cardiovascular system to postural stress[42] (*database 2*). The database includes physiological time series measured from 15 young healthy subjects monitored in the resting supine position (R) and in the 60° upright position (T) reached after a passive head-up tilt manoeuvre. The first analyzed time series contains 300 beats of RR intervals defined as above. The second time series contains the systolic arterial pressure (SAP), given as the local maxima of the the continuous photoplethysmographic arterial pressure signal (volume-clamp method) measured within each detected RR interval (see Fig. 4b). Further details on the experimental protocol, signal acquisition, and time series extraction procedure can be found in the reference paper[42].

3. *Cerebrovascular variability analysis*

Cerebrovascular interactions were investigated exploiting a historical database collected to study the response of cerebral autoregulation to postural stress[17] (*database 3*). The database includes physiological time series measured from 13 young healthy subjects monitored in the resting supine position (R) and in the 60° upright position (T) reached after a passive head-up tilt manoeuvre. Here, we analyzed time series of 250 beats of the mean arterial pressure (MAP) and mean cerebral blood flow velocity (MCBFV), obtained from the continuous photoplethysmographic arterial pressure signal (volume-clamp method) and cerebral blood flow velocity signal (transcranial doppler method); the time series samples were derived as the mean signal values measured between each pair of consecutive diastolic points (i.e., local minima, see Fig. 4c). Further details on the experimental protocol, signals acquisition, and time series extraction procedure can be found in the reference papers[17].

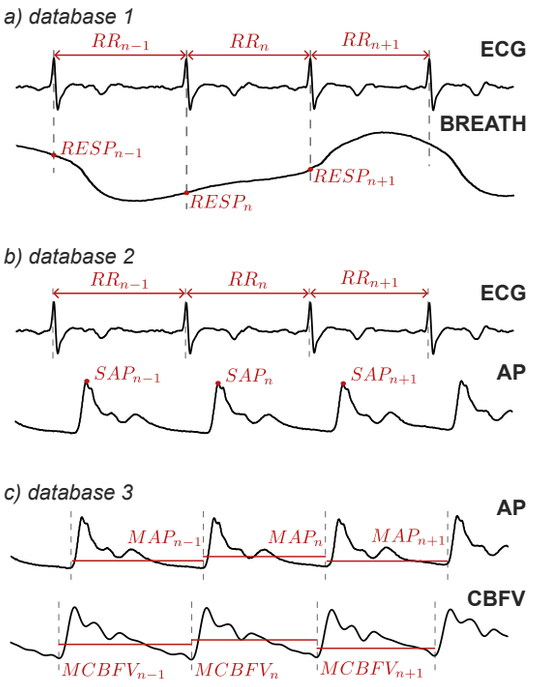

FIG. 4. Schematic representation of the procedure for extracting the time series from the physiological signals synchronously acquired in the three applications. (a) Cardiorespiratory variability analysis (database 1): the n^{th} RR value is the time interval between the n^{th} and the $(n+1)^{th}$ R peaks of the electrocardiogram (ECG), while the n^{th} RESP value is obtained sampling the respiration airflow signal (BREATH) in correspondence of the n^{th} R peak. (b) Cardiovascular variability analysis (database 2): the n^{th} SAP value is taken as the maximum value of the arterial pressure (AP) signal measured within the n^{th} RR interval. (c) Cerebrovascular variability analysis (database 3): from the arterial pressure (AP) and cerebral blood flow velocity (CBFV) signals, the n^{th} values of the mean AP (MAP) and mean CBFV (MCBFV) are obtained by averaging each signal within the n^{th} detected diastolic pulse interval defined as the time interval between two consecutive local minima.

B. Data analysis

The dynamic information measures composing the MIR were computed on the pairs of time series measured as described in the previous subsection, which were interpreted as realizations of the random processes $\{X,Y\}$ descriptive of cardiorespiratory interactions (X = RR, Y = RESP, *database 1*), cardiovascular interactions (X = RR, Y = SAP, *database 2*), and cerebrovascular interactions (X = MAP, Y = MCBFV, *database 3*). The two discretization approaches presented in Sect. II were employed to decompose the MIR either as the sum of the individual entropy rates of the two processes (i.e., H_X and H_Y) minus their joint entropy rate (i.e., $H_{X,Y}$), or as the sum of the two transfer entropies from one process to another (i.e., $T_{X\to Y}$ and $T_{Y\to X}$) plus the instantaneous information term (i.e., $I_{X\cdot Y}$).

In light of what reported in Sect. II D based on the results of the simulation study (see Sect. III B), we set the discretization parameters to $b=4$ and $m=1$ when implementing the binning approach, to limit the number of possible discrete states, and to $m=3$ when using the permutation approach, which is the minimum recommended to guarantee the variability of the discrete patterns[30]. The significance of each estimate of the MIR measure of its decomposition terms was assessed, for each pair of physiological time series, using surrogate data analysis similarly to what done in the simulation study.

Moreover, to assess the statistical significance of the variations of a given measures among different conditions, the following parametric tests were applied. As regards cardiorespiratory interactions, one-way analysis of variance (ANOVA) was applied, followed by a post-hoc paired Student's t-test with Bonferroni correction for multiple comparisons (n=3: SB vs. C10, SB vs. C15, SB vs. C20). As regards cardiovascular and cerebrovascular analyses, the paired Student's t-test was directly carried out between the two conditions under test. The use of parametric tests is justified by the fact that normality of the distributions was verified for all measures and all three databases through one-sample Kolmogorov-Smirnov test. All statistical tests were performed at a 5% significance level.

Finally, to assess the magnitude of the effect that a change in the experimental condition has on each analyzed index, the effect size was assessed using the Cohen's d index[43]. This index quantifies the difference between the means of the two distributions under analysis divided by the pooled standard deviation:

$$d = \frac{\bar{x}_1 - \bar{x}_2}{\sqrt{\frac{(n_1-1)s_1^2+(n_2-1)s_2^2}{n_1+n_2-2}}} \tag{9}$$

being $\bar{x}, s$, and n the mean, the standard deviation, and the number of samples (i.e., the number of subjects) of the two distributions under comparison, respectively. Usually, the effect size is considered small, medium, and large, if the absolute value of d is lower than 0.2, between 0.2 and 0.5, or higher than 0.8, respectively.

C. Results and Physiological Interpretation

1. *MIR analysis*

Fig. 5 reports the distribution of the MIR values estimated for the three datasets described above using the binning approach (a-c) and the permutation approach (d-f) to discretize the observed continuous-valued time series.

As regards cardiorespiratory interactions, for both approaches the ANOVA test highlighted significant variations across the phases of the breathing protocol. As reported in Table I, the p-value of the ANOVA test is far lower in the case of binning, for which the post-hoc paired tests evidence significantly higher values of $I_{RR;RESP}$ during paced breathing at 10 and 15 breaths/minute than during spontaneous breathing (Fig. 5a), also in association with a large effect size (Cohen's $|d| > 0.8$). A different trend is documented using the permutation method, for which a non-significant tendency to

lower MIR values during C15 and to higher MIR values during C20 is observed (Fig. 5d). Generally, the estimates obtained through the binning approach are significant for a larger number of subjects, although permutation-based method returns higher values.

With regard to cardiovascular interactions (Figs. 5b,e), no statistically significant differences in the MIR between RR interval and systolic pressure series are observed comparing the orthostatic stress and supine rest conditions. The estimates of $I_{RR;SAP}$ tend to exhibit opposite responses to the postural change, with tendency toward higher values using binning and toward lower values using permutations, both with a medium effect size (Table II).

Similar observations can be made for the cerebrovascular application, with absence of statistically significant differences in the MIR between mean cerebral flow velocity and arterial pressure series (Figs. 5c,d) and limited effect sizes (Table III) observed using both estimators.

Overall, these results suggest that the MIR measure is not very informative when applied to these datasets, as it does not discriminate the different physiological conditions and/or provides indications depending on the estimator adopted. In the following sections we will elaborate more on these aspects, decomposing the MIR in terms of complexity or causality measures and analyzing these measures in the three proposed physiological applications.

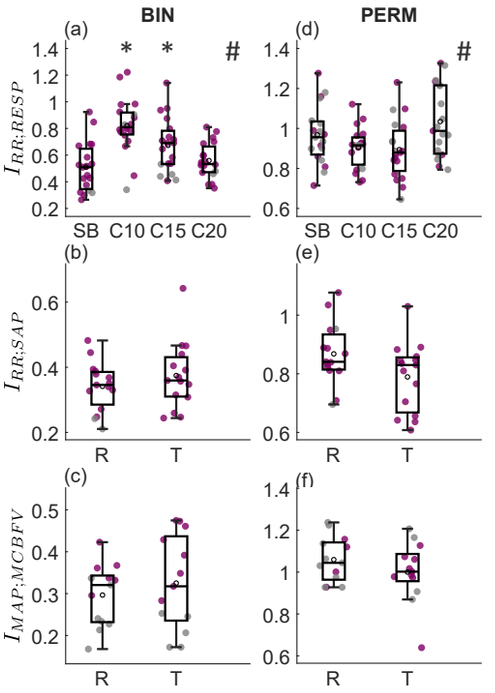

FIG. 5. Analysis of the MIR measure computed on pairs of physiological variability series. Panels report the boxplot distributions and individual values of the MIR computed: (a,d) on cardiorespiratory series (RR, RESP) analyzed during spontaneous breathing (SB) and controlled breathing at 10, 15, 20 breaths/minute (C10, C15, C20); (b,e) on cardiovascular series (RR, SAP) analyzed at rest (R) and after head-up tilt (T); (c,f) on cerebrovascular series (MAP, MCBFV) analyzed at rest (R) and after head-up tilt (T). The analysis was performed using the binning approach (a,b,c) or the permutation approach (d,e,f) for discretization. In each panel, colored and gray circles correspond to values deemed respectively as statistically significant and non-significant using surrogate data analysis; black open circles refer to the sample mean of each distribution. Statistically significant differences, cardiorespiratory series: #, p<0.05, ANOVA; *, p<0.05/3 SB vs. C10/C15/C20, paired t-test with Bonferroni correction; *, p<0.05, R vs. T, paired t-test.

2. *MIR decomposition: cardiorespiratory variability analysis*

Fig. 6 reports the distribution of the information measures composing the MIR computed for the RR and RESP time series using the binning (a-f) and permutation-based (g-l) approaches in the four phases of the paced breathing protocol.

Considering the decomposition evidencing the entropy rate measures computed via conditional entropy, the binning estimator reveals a tendency towards an increase of H_{RR} during paced breathing (Fig. 6a), with p-value of the ANOVA test slightly above the significance threshold (Table I); this was obsrved in the presence of stable values of H_{RESP} across conditions (Fig. 6b), and of lower values during C10 and higher values during C20 compared to SB for the joint entropy rate $H_{RR,RESP}$ (Fig. 6c). On the contrary, the permutation approach evidenced more consistently, when comparing the paced breathing conditions with SB, a significant decrease of all entropy rates during C10 and C15, and comparable or even higher values during C20 (Fig. 6g-i); the effect sizes are also larger when the entropy rate variations are assessed by permutations (Table I).

Physiologically, the lower entropy rates detected by the permutation method during C10 and C15, which can be taken as a marker of less complex RR and RESP dynamics, can be related to the mechanism of respiratory sinus arrhythmia (RSA), i.e., the variation of heart rate due to respiration. This mechanism is enhanced during forced ventilation at low breathing rates[44], while its effects compared with spontaneous breathing tend to be less pronounced when the respiratory rate increases[45]. Moreover, RSA and other cardiorespiratory control mechanisms, e.g., the cardio-ventilatory coupling and the respiratory stroke volume synchronization[46], are expected to elicit changes in the complexity of cardiac dynamics, associated with similar variations in the complexity of respiratory dynamics; we document that such changes are present as well when RR and RESP time series dynamics are evaluated together. On the other hand, we ascribe the lack of consistent changes in the entropy rate when the binning method is used to the limited exploitation of past values of the RR and RESP series in the evaluation of complexity ($m = 1$, compared with $m = 3$ used for the permutation method).

The different history length used for binning and permutation mentioned above plays probably a role also in the different trends observed considering the decomposition of the MIR between RR and RESP which evidences the causality measures computed via conditional mutual information. For this decomposition, the binning approach evidences higher

transfer entropies evaluated in both directions of interaction during C10 and C15 (Fig. 6d,e) along with stable values of the instantaneous information shared between RR and RESP (Fig. 6f). On the contrary, the permutation approach evidences rather stable values of the information transfer (see Fig. 6j,k, where only an increase of $T_{RESP\to RR}$ during C20 is detected) along with a decrease during C10 and C15 of the information shared instantaneously (see Fig. 6l, showing also that $I_{RR\cdot RESP}$ is barely significant). The patterns of information transfer evidenced by the permutation method are more consistent with those observed on the same dataset using both parametric and model-free estimators[47], and support the hypothesis that significant physiological changes in cardiac autonomic activity do not occur during supine paced breathing[44]. As regards the instantaneous information shared between RR and RESP, it should be noticed that its variations should be ascribed to directed effects from RESP to RR due to the way the RR and RESP time series were extracted from the physiological signals[47] (see Fig. 4).

3. *MIR decomposition: cardiovascular variability analysis*

Fig. 7 reports the distribution of the information measures composing the MIR computed for the RR and SAP time series measured at rest and during head-up tilt using the binning (a-f) and permutation-based (g-l) approaches.

In this application, the binning and permutation approaches for the discretization of the observed time series lead to similar results, as documented in Fig. 7. The MIR decomposition computed via conditional entropy shows how the orthostatic stress dampens the complexity of cardiovascular dynamics, as documented by the statistically significant decrease of the joint entropy rate of RR and SAP (Fig. 7c,i). The decrease is mainly driven by the simplification of the cardiac dynamics evidenced by the drop of the entropy rate of RR (Fig. 7a,g), in the presence of an unchanged entropy rate of SAP (Fig. 7b,h). These trends are detected more evidently using the binning estimator, which yields lower p-values and higher effect sizes in the comparison between the rest and tilt conditions (Table II). Physiologically, these results find large confirmation in the literature and are related to the tilt-induced activation of the sympathetic nervous system which tends to simplify the cardiac dynamics, yielding a reduction of the complexity of short-term heart rate variability[6,16,48].

As regards the causality measures computed via conditional mutual information, the most straightforward result is the increase of the transfer entropy from SAP to RR moving from rest to tilt, which is documented by both binning and permutation approaches (Fig. 7e,k). The information transfer along the opposite direction from RR to SAP shows a significant decrease during tilt, which is detected using the permutation method (Fig. 7j) but not using the binning method (Fig. 7d). According to both discretization approaches, the information shared instantaneously by the two series is rather low and significant in a few subjects, and tends to decrease significantly while moving from rest to tilt (Fig. 7f,l). These results show how the information transferred within the RR-SAP closed-

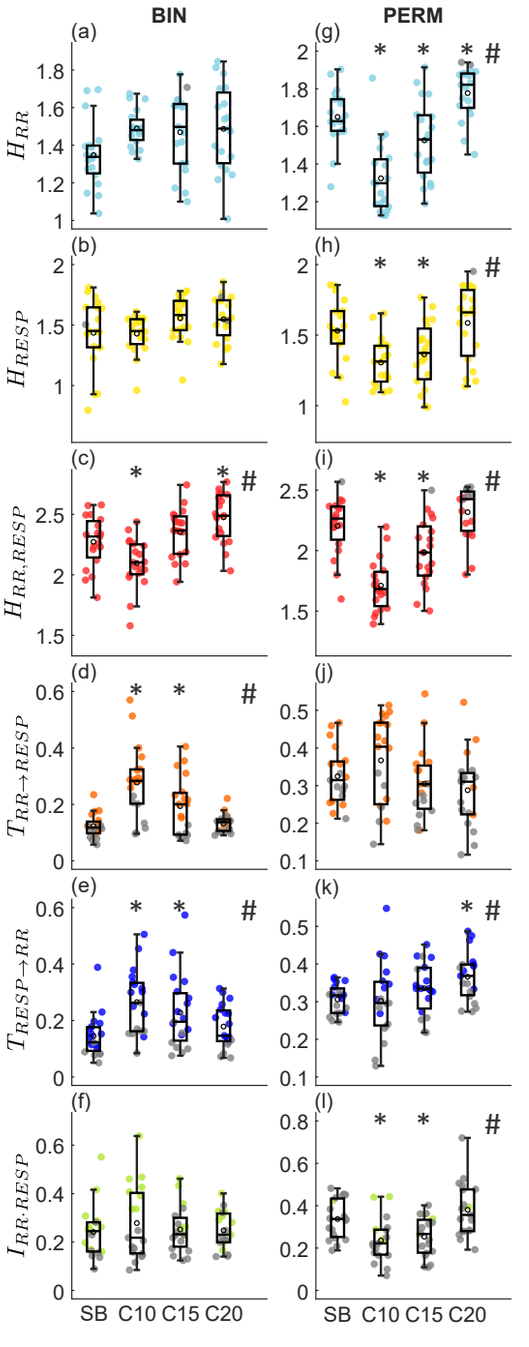

FIG. 6. MIR decomposition of cardiorespiratory interactions (*database 1*). Panels report the boxplot distributions and individual values of the MIR decomposition evidencing conditional entropy terms (Eq. (3), H_{RR}, H_{RESP}, $H_{RR,RESP}$) or the MIR decomposition evidencing conditional mutual information terms (Eq. (4), $T_{RR\to RESP}$, $T_{RESP\to RR}$, $I_{RR\cdot RESP}$), computed during spontaneous breathing (SB) and controlled breathing at 10, 15, 20 breaths/minute (C10, C15, C20) using the binning approach (a-f) or the permutation approach (g-l) for discretization. In each panel, colored and gray circles correspond to values deemed respectively as statistically significant and non-significant using surrogate data analysis; black open circles refer to the sample mean of each distribution. Statistically significant differences: #, p<0.05, ANOVA; *, p<0.05/3 SB vs. C10/C15/C20, paired t-test with Bonferroni correction.

TABLE I. Results of statistical analyses (ANOVA and uncorrected t-test p-values) and effect size (Cohen's d) performed on cardiorespiratory variability series (*database 1*). Values in bold indicate statistically significant ANOVA ($p < 0.05$), post-hoc t-test p-values after Bonferroni correction ($n = 3$) and large ($|d| > 0.8$) effect sizes. t-test p-values are not in bold if the ANOVA test is not significant.

Measure	Type	p ANOVA	p SB-C10	d SB-C10	p SB-C15	d SB-C15	p SB-C20	d SB-C20
H_{RR}	binning	0.0568	0.0008	**-1.005**	0.0114	-0.645	0.0141	-0.688
	permutation	**<10^{-9}**	**<10^{-7}**	**1.908**	**0.0115**	0.683	**0.0046**	**-0.878**
H_{RESP}	binning	0.1136	0.9331	0.028	0.0901	-0.496	0.1724	-0.458
	permutation	**0.0005**	**0.0012**	**1.136**	**0.0110**	0.731	0.3412	-0.218
$H_{RR,RESP}$	binning	**<10^{-5}**	**0.0051**	**0.830**	0.1890	-0.383	**0.0058**	**-0.970**
	permutation	**<10^{-10}**	**<10^{-6}**	**2.186**	**0.0019**	**0.853**	0.0874	-0.498
$T_{RR\to RESP}$	binning	**<10^{-6}**	**0.0003**	**-1.617**	**0.0126**	**-0.901**	0.5162	-0.235
	permutation	0.0838	0.1689	-0.424	0.4190	0.235	0.1667	0.421
$T_{RESP\to RR}$	binning	**0.0028**	**0.0041**	**-1.245**	**0.0080**	-0.780	0.1055	-0.443
	permutation	**0.0260**	0.8766	0.051	0.0788	-0.529	**0.0015**	**-1.128**
$I_{RR\cdot RESP}$	binning	0.7551	0.2294	-0.279	0.6785	-0.102	0.7901	-0.071
	permutation	**0.0001**	**0.0137**	**1.049**	**0.0138**	**0.895**	0.2093	-0.387
$I_{RR;RESP}$	binning	**<10^{-5}**	**0.0002**	**-1.573**	**0.0056**	**-0.843**	0.2540	-0.305
	permutation	**0.0141**	0.0952	0.500	0.1111	0.502	0.1692	-0.412

TABLE II. Results of statistical analyses and effect size (Cohen's d) performed on cardiovascular variability series (*database 2*). Values in bold indicate statistically significant p-values and large ($|d| > 0.8$) effect sizes.

Measure	Type	p R-T	d R-T
H_{RR}	binning	**<10^{-4}**	**2.103**
	permutation	**0.0053**	**1.166**
H_{SAP}	binning	0.9214	-0.030
	permutation	0.0554	0.704
$H_{RR,SAP}$	binning	**0.0006**	**1.563**
	permutation	**0.0012**	**1.370**
$T_{RR\to SAP}$	binning	0.9916	-0.003
	permutation	**0.0267**	**0.766**
$T_{SAP\to RR}$	binning	**0.0002**	**-1.515**
	permutation	**0.0260**	**-1.124**
$I_{RR\cdot SAP}$	binning	**0.0289**	0.782
	permutation	**0.0027**	**1.332**
$I_{RR;SAP}$	binning	0.1895	-0.366
	permutation	0.1030	0.705

loop is balanced along the two directions of interaction in the resting supine position, and becomes unbalanced in the upright position as a consequence of the well-known tilt-induced activation of the baroreflex feedback from SAP to RR accompanied by a weakening of the mechanical feedforward from RR to SAP[6,42,49].

4. *MIR decomposition: cerebrovascular variability analysis*

Fig. 8 depicts the distribution of the information measures composing the MIR computed for the MAP and MCBFV time series measured during the rest and tilt conditions using the binning (a-f) and permutation-based (g-l) approaches.

The MIR decomposition based on conditional entropy measures performed with the permutation approach evidences a statistically significant decrease of the entropy rate of MAP variability (Fig. 8g) and of the joint entropy rate of MAP and MCBFV (Fig. 8i) moving from rest to tilt, while the individual entropy rate of MCBFV does not change between the two conditions (Fig. 8h). This response to postural stress, which could not be detected using the binning estimator (Figs. 8a-c), is indicative of an increase of the predictability of the cerebrovascular dynamics, which is driven by a larger predictability of MAP but not MCBFV. As regards the MIR decomposition based on conditional mutual information, all its terms estimated either via the binning or via the permutation approach are not statistically signifcant in several subjects and do not change significantly moving from rest to tilt (Figs. 8d-f, 8j-l). This result may indicate the presence of low coupling between MAP and MCBFV, or the limited ability of the considered discretization strategies to detect such coupling in the analyzed dataset.

The results presented above are in agreement with the hypothesis that the physiological mechanisms related to cerebrovascular autoregulation, which are responsible for regulating the cerebral blood flow and maintaining it almost constant independently from changes in the systemic arterial pressure[50,51], are preserved after postural stress. Similar findings were obtained by recent studies suggesting that the increased sympathetic nerve activity occurring with the postural challenge leads to a reduction of MCBFV, but not to changes in its variability or predictability, and does not alter significantly the coupling between MCBFV and MAP[17,26] .

V. DISCUSSION

The purpose of this work was to assess the effectiveness of model-free symbolization methods for investigating coupled physiological dynamics through the MIR measure and its decomposition terms. A comparative investigation of symbolic methods based on binning and permutation for the

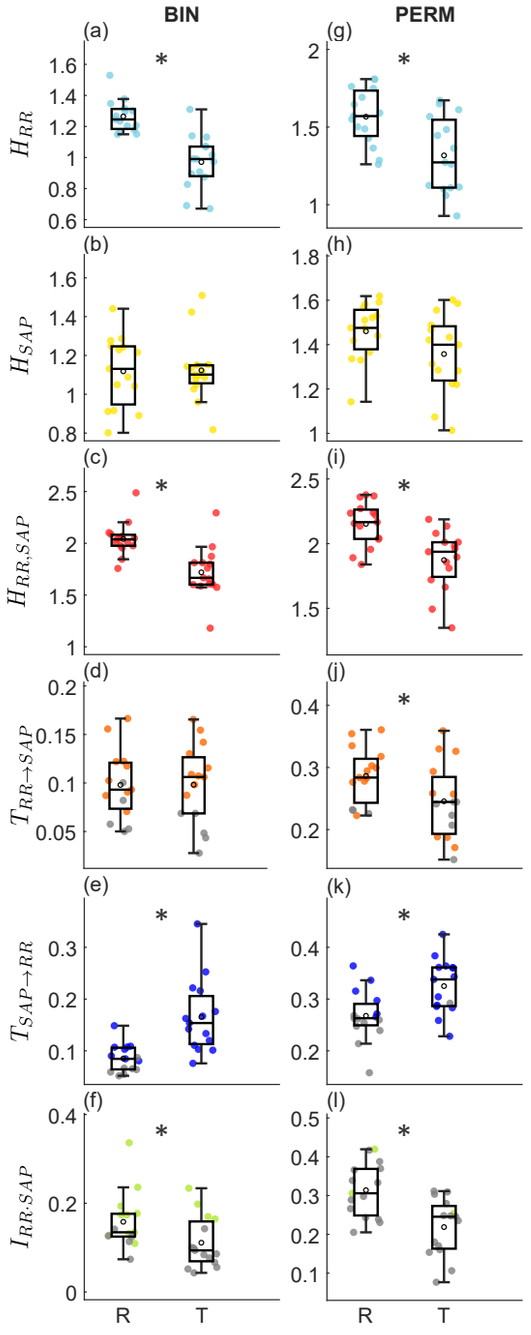

FIG. 7. MIR decomposition of cardiovascular interactions (*database 2*). Panels report the boxplot distributions and individual values of the MIR decomposition evidencing conditional entropy terms (Eq. (3), H_{RR}, H_{SAP}, $H_{RR,SAP}$) or the MIR decomposition evidencing conditional mutual information terms (Eq. (4), $T_{RR\to SAP}$, $T_{SAP\to RR}$, $I_{RR;SAP}$), computed in the resting supine position (R) and in the upright position during tilt (T) using the binning approach (a-f) or the permutation approach (g-l) for discretization. In each panel, colored and gray circles correspond to values deemed respectively as statistically significant and non-significant using surrogate data analysis; black open circles refer to the sample mean of each distribution. Statistically significant differences: *, p<0.05 R vs. T, paired t-test.

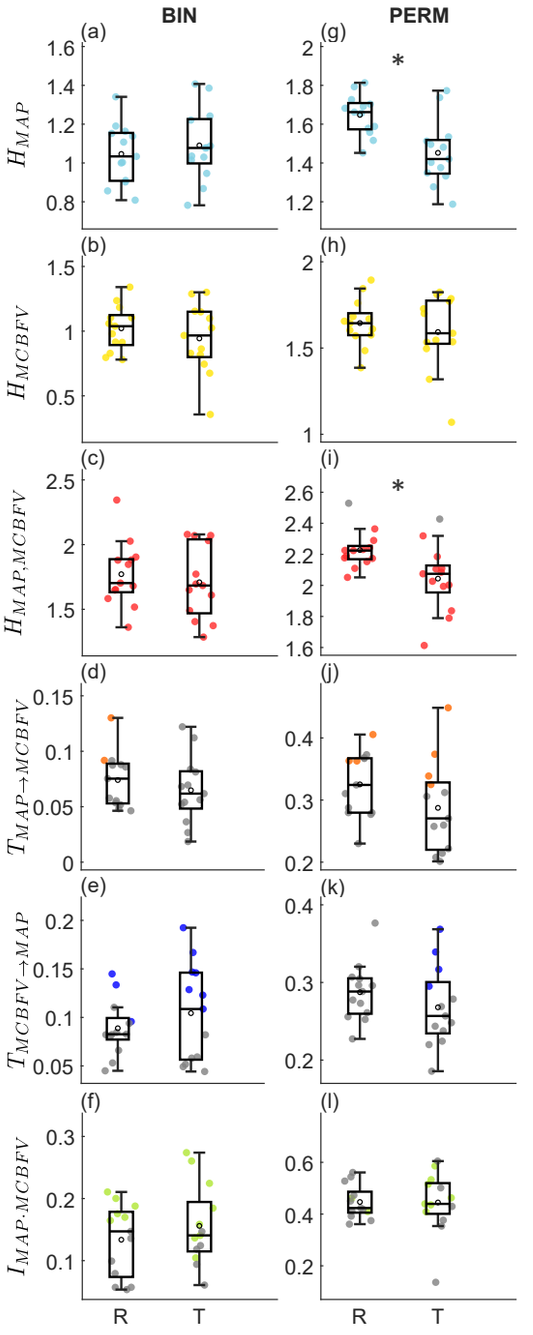

FIG. 8. MIR decomposition of cerebrovascular interactions (*database 3*). Panels report the boxplot distributions and individual values of the MIR decomposition evidencing conditional entropy terms (Eq. (3), H_{MAP}, H_{MCBFV}, $H_{MAP,MCBFV}$) or the MIR decomposition evidencing conditional mutual information terms (Eq. (4), $T_{MAP\to MCBFV}$, $T_{MCBFV\to MAP}$, $I_{MAP;MCBFV}$), computed in the resting supine position (R) and in the upright position during tilt (T) using the binning approach (a-f) or the permutation approach (g-l) for discretization. In each panel, colored and gray circles correspond to values deemed respectively as statistically significant and non-significant using surrogate data analysis; black open circles refer to the sample mean of each distribution. Statistically significant differences: *, p<0.05 R vs. T, paired t-test.

TABLE III. Results of statistical analyses and effect size (Cohen's d) performed on cerebrovascular variability series (*database 3*). Values in bold indicate statistically significant p-values and large ($|d| > 0.8$) effect sizes.

Measure	Type	p R-T	d R-T
H_{MAP}	binning	0.4028	-0.260
	permutation	**0.0015**	**1.404**
H_{MCBFV}	binning	0.3992	0.346
	permutation	0.3738	0.261
$H_{MAP,MVBFV}$	binning	0.5355	0.235
	permutation	**0.0020**	**1.060**
$T_{MAP\to MCBFV}$	binning	0.3854	0.334
	permutation	0.1701	0.597
$T_{MCBFV\to MAP}$	binning	0.3186	-0.381
	permutation	0.2836	0.434
$I_{MAP\cdot MCBFV}$	binning	0.2608	-0.366
	permutation	0.9519	0.020
$I_{MAP;MCBFV}$	binning	0.4185	-0.300
	permutation	0.2956	0.462

information-theoretic investigation of dynamic coupling measures was performed both on simulated nonlinear coupled systems and on cardiorespiratory, cardiovascular, and cerebrovascular time series. Our results support the feasibility of these estimates to evaluate complex dynamics and dynamical interactions, and delineate advantages and drawbacks of each method.

A. Estimating the decomposition of the Mutual Information Rate via model-free discretization methods

While the theoretical formulation of the MIR (Eq. (1)) and of its decompositions evidencing conditional entropy measures (Eq. (3)) and conditional mutual information measures (Eq. (4)) are well-defined and long-known[18,20–22], the practical estimation of all these measures from finite-length realizations of coupled random processes is far from trivial. A main issue is related to the fact that both the MIR and the terms of its decomposition are defined for infinite-dimensional variables sampling the whole temporal evolution of the analyzed processes (see Eqs. (1,2,5)). This issue is often addressed using linear parametric models to describe the interactions between the present and past states of the processes. In such a case, under the assumption of Gaussian multivariate process the information dynamical measures are directly derived from the covariance matrices of the processes. Thus, the conditional entropy of the present of a process given its past and/or the past of the other process is defined in terms of the variance of the prediction error of a linear regression of the present variable on the past variables. The relations connecting e.g. the entropy rate to the prediction error variance[27] and the transfer entropy to Granger causality[52], can be practically computed even on short time series accounting also for long memory effects by employing parametric approaches which involve the solution of the Yule-Walker equations[47,53] or the formulation of state space models[24,54], or even exploiting the relations between time-domain and spectral measures[20,26,55].

However, when a model-free analysis is required to account for possible nonlinear interactions which invalidate the Gaussian assumption, the only viable approach is to work under the Markov property. This allows to reduce drastically the length of the analyzed dynamical patterns by setting finite values (at an order depending on the time series length) for the parameter related to memory effects (k in Eqs. (1,2) and m in the approximation of the measures in Eq. (5)) and assuming that longer-memory effects are negligible. In model-free approaches like those based on discretization used in this work, the use of short memories is necessary to limit the curse of dimensionality[37], i.e., the inability to make sense of a small set of points in a high dimensional space. In particular, estimation of probability distributions computed for high-dimensional variables observed from short time series is problematic leading to highly biased entropy estimates and entropy rate estimates that decrease toward zero as the memory of the process increases[25,29]. Moreover, an additional bias results from the combination of entropy terms computed on variables spanning spaces of different dimensions[56]; this issue is exacerbated in the estimation of the MIR, as implemented here, which results combining several entropy terms estimated independently from one another. In contrast to the binning and permutation entropy estimates, the nearest neighbor estimate corrects for this bias by taking the spaces regarding the different variables in the entropy terms as projections of the largest space[56,57].

In this work, the above issues are reflected by the necessity to choose values of the estimator parameters which limit the dimension of the spaces populated by the points formed by present and past values of the analyzed processes. Indeed, as shown in Sect. III B on the simulated coupled Hènon maps, working with long memory effects and/or several quantization levels (e.g., $b = 3$, $m = 2$ for binning, and $m = 4$ for permutation) is problematic under the challenging conditions of short data lengths. The main issue is the too large number of possible patterns, which reduces the significance of the obtained estimates. On the other hand, the reverse choice (e.g., $b = 2$, $m = 3$ for binning, and $m = 2$ for permutation) results in the inability of the estimator to fully resolve the dynamics of the process. Therefore, in view of the simulation results and to reach compromise between accuracy in the representation of the dynamics and reliability of the estimates, in the applications to physiological time series the memory length was set to $m = 3$ for the permutation approach and to $m = 1$ for the binning approach, for which a number of quantization levels $b = 4$ was also chosen.

While the results obtained for the various MIR terms are physiologically plausible in all the three application contexts considered, some of our findings suggest caution in the use of these parameters or to seek for alternative ways to set them (e.g., non-uniform embedding[57–59]). In fact, the lack of statistical significance of $T_{X\to Y}$, $T_{Y\to X}$, $I_{X\cdot Y}$ and $I_{X;Y}$ observed in many subjects in all applications can be ascribed to the combination of biases obtained working with high dimensional spaces and small data size. As also expected from the results reported in the simulation study, the chosen parameters

make this behavior most visible for the permutation-based estimates of instantaneous causality and MIR measures, since this is the highest-dimensional case for which the empirical rule suggested to limit the bias is not respected. In the case of binning, the necessity of setting low values of m and b in order to keep the alphabet sizes low and comparable for the different entropy measures appearing in (5) is likely the reason for some unexpected behaviors of the MIR terms, as we will discuss in the next section.

B. Comparison of binning and permutation-based approaches

The binning method is perhaps the most intuitive method to compute entropy measures via discretization, and has been used in numerous previous works analyzing short-term physiological interactions[25,29,58]. As mentioned before, in order to mitigate the issue related to the number of symbolic patterns used to describe the observed dynamics, a low number of quantization levels ($b = 4$) and a limited embedding dimension ($m = 1$) have been set to deal with the small size of the analyzed series (250-300 points). These choices have the consequence to limit the degree of detail in analyzing the amplitude variations and the time-lagged interactions occurring within and between the analyzed processes, possibly impairing the ability to detect subtle changes and long-memory effects. On the other hand, the permutation method allows to work with a number of symbolized patterns which is typically much lower than that used for binning[35,36]. This occurs because, given the same embedding dimension, the rank-ordering procedure implicitly leads to a much lower number of patterns than the quantization procedure. Considering this aspect, which is expected to improve the estimation of probability distributions and thus of entropy measures, a higher embedding dimension ($m = 3$) has been set when applying the permutation-based method, which allows to achieve a more detailed description of the memory effects.

The results achieved on the simulated system demonstrate how the selection of the discretization parameters reflects the effectiveness of the information measures in revealing variations of the coupling between the systems. When comparing the two discretization approaches, it can be observed that the sensitivity to the coupling parameter of the MIR decompositions terms (i.e., $I_{X;Y}$, H_Y, $T_{X\to Y}$ and $I_{X\cdot Y}$) is larger when evaluated with the permutation-based method. This result evidences how the rank ordering approach generally can achieve a more accurate description of complex intertwined dynamics. Importantly, the same remarks can be made regarding the detection of changes across physiological conditions, to an extent depending on the application considered.

In cardiorespiratory variability analysis, the fact that RSA is more evident during paced breathing at low breathing frequency[44] is reflected by an increase of the predictability and a decrease of the complexity of heart rate variability compared to spontaneous breathing, and this effect becomes less pronounced as the breathing rate increases[47]. Conversely, no evident changes in the information transferred between heart rate and respiration variability have been detected using either linear and nonlinear measures of Granger causality[47]. These patterns were detected in our analysis using permutations but not using the binning approach. This difference may be ascribed to the utilization of a too short embedding dimension, which prevents the binning approach to detect the decreased complexity of RR and RESP during slow paced breathing, possibly because the memory effects occur at lags $m > 1$. A confirmation of this comes from the fact that, when measures working in higher dimensions such as the joint entropy rate or the transfer entropies were computed, significant variations during slow paced breathing were detected also by the binning estimator (Fig. 6); in the case of the transfer entropies the significant variation is likely misleading and reflects more the use of a larger dimension than a physiological behavior. These considerations were supported repeating the analysis of cardiorespiratory interactions based on binning while using higher values for m: in this way we observed patterns of information dynamics more adherent to those already found in the literature[47] and in this study using the permutation method (results not shown).

As regards the analysis of cardiovascular interactions, we found that the binning approach leads to results similar to those achieved by the permutation method and by other linear and nonlinear measures of complexity, coupling and causality[11,42,58,60]. Here, our results evidenced that both permutation and binning methods are able to reflect marked variations in the cardiovascular dynamics occurring during postural stress, such as the drop in the complexity of RR and the rise of the causal coupling from SAP to RR (Fig. 7). The only physiological effect that was not detected by the binning method is the decrease of $T_{RR\to SAP}$ during tilt. Again, this could be ascribed to the limited memory used to evaluate the past dynamics of the process. In fact, lag-specific approaches employed on the same dataset to assess causal RR-SAP interactions suggested that the transfer of information occurs primarily at lags 0 and 1 in the direction from SAP to RR and at lag 2 in the opposite direction from RR to SAP[15,58].

The observations above point out that the permutation approach yields results that are more in line with the literature than those provided by the binning approach, mainly as result of the fact that the more parsimonious representation of the discretized dynamic patterns allows to explore higher-dimensional spaces. Nevertheless, the use of $m = 3$ yields a number of patterns which is lower than the time series length when the individual entropy rates or transfer entropies are estimated, but approximately double the series length when the measures involving the highest dimensional spaces are involved. This size for the alphabets turned out to be problematic particularly for the instantaneous information shared by the processes, which resulted barely significant in all applications when computed using permutations. Moreover, the permutation-based method suffers from some limitations that may influence its ability to capture accurately the analyzed dynamic interactions. First, this method is affected by a bias due to the presence of equal values inside the patterns which can confound the estimation[61]. While in our work we decided that equal values are ranked according to their temporal order, other choices can be made but none of them actually limits the

bias in the estimation of different quantities. With regard to this, a modified permutation-entropy has been proposed which maps equal values to the same symbols[62], so as to take into account the presence of equal values within the patterns that may have physiological significance, but this leads to an increase of the dimension of the space visited by the discrete variables and thus to the above-discussed matters. The second constraint of the permutation method is the lack of information related to differences in the amplitude among the time series samples, which may represent a limitation in following some physiological nonlinear behaviors[63], but also in the presence of noise[60]. In fact, it was found that permutation-based measures are more susceptible to broad-band noise especially when working with low signal-to-noise ratio and short time series length. On the other hand, not accounting for signal amplitudes makes the permutation method more robust in the presence of nonstationarities[30,36]. In particular, the presence of amplitude artifacts and slow trends, which is highly detrimental for most entropy estimators[32], should have a lower impact on procedures which discard the amplitude values apart from considering their rank. This aspect may be relevant in our application to cerebrovascular dynamics, where the occurrence of physiological oscillations at low and very low frequency trends[26] can be one of the reasons for the inability of the binning method to capture the complexity changes of mean arterial pressure evoked by tilt.

C. Conclusion and future investigations

This study points out the feasibility of investigating short-term interactions in bivariate physiological time series by means of model-free estimators of the mutual information rate and of its constituent terms implemented via discretization strategies. The most critical aspect identified by our results is the need to set the analysis parameters to values that limit the curse of dimensionality. From this point of view, the permutation approach to discretization based on rank ordering is preferable, as it yields a more parsimonious representation of the discretized patterns representing the observed dynamics. Still, the use of permutations becomes problematic when implemented in high-dimensional spaces. As regards the binning approach, we suggest that it can be used with the standard setting of the embedding and quantization parameters for estimating the entropy rate of individual time series, while shorter memories and heavier coarse graining should be used to reliably assess the higher-dimensional terms of the MIR decomposition.

Further work is envisaged to explore more in depth the performance of model-free approaches for the estimation of dynamic information measures from short realizations of multivariate time series, and to develop improved estimators. In particular, future studies should assess more systematically the behaviour of binning and permutation methods in comparison with approaches not based on discretization, developed using either model-free[56] or model-based[6] estimators. In parallel, strategies for dimension reduction[57,59] or automatic parameter selection[64] should be explored to optimize the embedding of multivariate time series limiting the curse of dimensionality. In perspective, the combination of improved entropy estimators and optimized methods for parameter selection can open new avenues for the model-free assessment of the information processed by network systems, even beyond the framework of pairwise interactions[24,65].

ACKNOWLEDGMENTS

This work was supported by the project "Sensoristica intelligente, infrastrutture e modelli gestionali per la sicurezza di soggetti fragili" (4FRAILTY), funded by Italian Ministry of Education, University and Research (MIUR), PON R&I grant ARS0100345, CUP B76G18000220005. R.P. is partially supported by European Social Fund (ESF)—Complementary Operational Programme (POC) 2014/2020 of the Sicily Region.

DATA AVAILABILITY STATEMENT

The data presented in this study will be made available upon reasonable request from the corresponding author.

REFERENCES

[1] N. F. Rulkov, M. M. Sushchik, L. S. Tsimring, and H. D. Abarbanel, "Generalized synchronization of chaos in directionally coupled chaotic systems," Physical Review E **51**, 980 (1995).
[2] J. Arnhold, P. Grassberger, K. Lehnertz, and C. E. Elger, "A robust method for detecting interdependences: application to intracranially recorded eeg," Physica D: Nonlinear Phenomena **134**, 419–430 (1999).
[3] L. Faes, A. Porta, and G. Nollo, "Mutual nonlinear prediction as a tool to evaluate coupling strength and directionality in bivariate time series: comparison among different strategies based on k nearest neighbors," Physical Review E **78**, 026201 (2008).
[4] K. Li, L. Guo, J. Nie, G. Li, and T. Liu, "Review of methods for functional brain connectivity detection using fmri," Computerized medical imaging and graphics **33**, 131–139 (2009).
[5] A. Bashan, R. P. Bartsch, J. Kantelhardt, S. Havlin, P. C. Ivanov, *et al.*, "Network physiology reveals relations between network topology and physiological function," Nature communications **3**, 1–9 (2012).
[6] L. Faes, G. Nollo, and K. H. Chon, "Assessment of granger causality by nonlinear model identification: application to short-term cardiovascular variability," Annals of biomedical engineering **36**, 381–395 (2008).
[7] S. L. Bressler and A. K. Seth, "Wiener–granger causality: a well established methodology," Neuroimage **58**, 323–329 (2011).
[8] J. T. Lizier, *The local information dynamics of distributed computation in complex systems* (Springer Science & Business Media, 2012).
[9] M. Wibral, J. T. Lizier, and V. Priesemann, "Bits from brains for biologically inspired computing," Frontiers in Robotics and AI **2**, 5 (2015).
[10] D. Widjaja, A. Montalto, E. Vlemincx, D. Marinazzo, S. Van Huffel, and L. Faes, "Cardiorespiratory information dynamics during mental arithmetic and sustained attention," PLoS One **10**, e0129112 (2015).
[11] M. Javorka, J. Krohova, B. Czippelova, Z. Turianikova, Z. Lazarova, R. Wiszt, and L. Faes, "Towards understanding the complexity of cardiovascular oscillations: Insights from information theory," Computers in biology and medicine **98**, 48–57 (2018).
[12] M. Wibral, J. T. Lizier, S. Vögler, V. Priesemann, and R. Galuske, "Local active information storage as a tool to understand distributed neural information processing," Frontiers in neuroinformatics **8**, 1 (2014).

[13]L. Faes, M. A. Pereira, M. E. Silva, R. Pernice, A. Busacca, M. Javorka, and A. P. Rocha, "Multiscale information storage of linear long-range correlated stochastic processes," Physical Review E **99**, 032115 (2019).
[14]R. Vicente, M. Wibral, M. Lindner, and G. Pipa, "Transfer entropy—a model-free measure of effective connectivity for the neurosciences," Journal of computational neuroscience **30**, 45–67 (2011).
[15]L. Faes, D. Marinazzo, A. Montalto, and G. Nollo, "Lag-specific transfer entropy as a tool to assess cardiovascular and cardiorespiratory information transfer," IEEE Transactions on Biomedical Engineering **61**, 2556–2568 (2014).
[16]L. Faes, M. Gómez-Extremera, R. Pernice, P. Carpena, G. Nollo, A. Porta, and P. Bernaola-Galván, "Comparison of methods for the assessment of nonlinearity in short-term heart rate variability under different physiopathological states," Chaos: An Interdisciplinary Journal of Nonlinear Science **29**, 123114 (2019).
[17]V. Bari, B. De Maria, C. E. Mazzucco, G. Rossato, D. Tonon, G. Nollo, L. Faes, and A. Porta, "Cerebrovascular and cardiovascular variability interactions investigated through conditional joint transfer entropy in subjects prone to postural syncope," Physiological Measurement **38**, 976 (2017).
[18]T. E. Duncan, "On the calculation of mutual information," SIAM Journal on Applied Mathematics **19**, 215–220 (1970).
[19]E. Bianco-Martinez, N. Rubido, C. G. Antonopoulos, and M. Baptista, "Successful network inference from time-series data using mutual information rate," Chaos: An Interdisciplinary Journal of Nonlinear Science **26**, 043102 (2016).
[20]D. Chicharro, "On the spectral formulation of granger causality," Biological cybernetics **105**, 331–347 (2011).
[21]M. Baptista and J. Kurths, "Transmission of information in active networks," Physical Review E **77**, 026205 (2008).
[22]G. Mijatovic, Y. Antonacci, T. Loncar-Turukalo, L. Minati, and L. Faes, "An information-theoretic framework to measure the dynamic interaction between neural spike trains," IEEE Transactions on Biomedical Engineering **68**, 3471–3481 (2021).
[23]G. Mijatovic, R. Pernice, A. Perinelli, Y. Antonacci, A. Busacca, M. Javorka, L. Ricci, and L. Faes, "Measuring the rate of information exchange in point-process data with application to cardiovascular variability," Front. Netw. Physiol. 1: 765332. doi: 10.3389/fnetp (2022).
[24]L. Faes, G. Mijatovic, Y. Antonacci, R. Pernice, C. Barà, L. Sparacino, M. Sammartino, A. Porta, D. Marinazzo, and S. Stramaglia, "A new framework for the time-and frequency-domain assessment of high-order interactions in networks of random processes," IEEE Transactions on Signal Processing (2022).
[25]A. Porta, G. Baselli, D. Liberati, N. Montano, C. Cogliati, T. Gnecchi-Ruscone, A. Malliani, and S. Cerutti, "Measuring regularity by means of a corrected conditional entropy in sympathetic outflow," Biological cybernetics **78**, 71–78 (1998).
[26]R. Pernice, L. Sparacino, V. Bari, F. Gelpi, B. Cairo, G. Mijatovic, Y. Antonacci, D. Tonon, G. Rossato, M. Javorka, *et al.*, "Spectral decomposition of cerebrovascular and cardiovascular interactions in patients prone to postural syncope and healthy controls," Autonomic Neuroscience , 103021 (2022).
[27]A. B. Barrett, L. Barnett, and A. K. Seth, "Multivariate granger causality and generalized variance," Physical Review E **81**, 041907 (2010).
[28]H. Azami, L. Faes, J. Escudero, A. Humeau-Heurtier, and L. E. Silva, "Entropy analysis of univariate biomedical signals: Review and comparison of methods," Frontiers in Entropy Across the Disciplines: Panorama of Entropy: Theory, Computation, and Applications , 233–286 (2020).
[29]L. Faes and A. Porta, "Conditional entropy-based evaluation of information dynamics in physiological systems," in *Directed information measures in neuroscience* (Springer, 2014) pp. 61–86.
[30]C. Bandt and B. Pompe, "Permutation entropy: a natural complexity measure for time series," Physical review letters **88**, 174102 (2002).
[31]T. M. Cover, *Elements of information theory* (John Wiley & Sons, 1999).
[32]W. Xiong, L. Faes, and P. C. Ivanov, "Entropy measures, entropy estimators, and their performance in quantifying complex dynamics: Effects of artifacts, nonstationarity, and long-range correlations," Physical Review E **95**, 062114 (2017).
[33]M. Staniek and K. Lehnertz, "Symbolic transfer entropy," Physical review letters **100**, 158101 (2008).
[34]A. M. Unakafov and K. Keller, "Conditional entropy of ordinal patterns," Physica D: Nonlinear Phenomena **269**, 94–102 (2014).
[35]D. Kugiumtzis, "Transfer entropy on rank vectors," Journal of Nonlinear Systems and Applications **73**, 81 (2012).
[36]D. Kugiumtzis, "Partial transfer entropy on rank vectors," The European Physical Journal Special Topics **222**, 401–420 (2013).
[37]J. Runge, J. Heitzig, V. Petoukhov, and J. Kurths, "Escaping the curse of dimensionality in estimating multivariate transfer entropy," Physical review letters **108**, 258701 (2012).
[38]J. Theiler, S. Eubank, A. Longtin, B. Galdrikian, and J. D. Farmer, "Testing for nonlinearity in time series: the method of surrogate data," Physica D: Nonlinear Phenomena **58**, 77–94 (1992).
[39]R. Q. Quiroga, A. Kraskov, T. Kreuz, and P. Grassberger, "Performance of different synchronization measures in real data: a case study on electroencephalographic signals," Physical Review E **65**, 041903 (2002).
[40]M. Wiesenfeldt, U. Parlitz, and W. Lauterborn, "Mixed state analysis of multivariate time series," International Journal of Bifurcation and Chaos **11**, 2217–2226 (2001).
[41]A. Porta, T. Bassani, V. Bari, and S. Guzzetti, "Granger causality in cardiovascular variability series: Comparison between model-based and model-free approaches," in *2012 Annual International Conference of the IEEE Engineering in Medicine and Biology Society* (IEEE, 2012) pp. 3684–3687.
[42]G. Nollo, L. Faes, A. Porta, R. Antolini, and F. Ravelli, "Exploring directionality in spontaneous heart period and systolic pressure variability interactions in humans: implications in the evaluation of baroreflex gain," American Journal of Physiology-Heart and Circulatory Physiology **288**, H1777–H1785 (2005).
[43]J. Cohen, *Statistical power analysis for the behavioral sciences* (Routledge, 2013).
[44]J. P. Saul, R. D. Berger, M. Chen, and R. J. Cohen, "Transfer function analysis of autonomic regulation. ii. respiratory sinus arrhythmia," American Journal of Physiology-Heart and Circulatory Physiology **256**, H153–H161 (1989).
[45]H.-S. Song and P. M. Lehrer, "The effects of specific respiratory rates on heart rate and heart rate variability," Applied psychophysiology and biofeedback **28**, 13–23 (2003).
[46]M. Elstad, E. L. O'Callaghan, A. J. Smith, A. Ben-Tal, and R. Ramchandra, "Cardiorespiratory interactions in humans and animals: rhythms for life," American Journal of Physiology-Heart and Circulatory Physiology **315**, H6–H17 (2018).
[47]L. Faes, A. Porta, and G. Nollo, "Information decomposition in bivariate systems: theory and application to cardiorespiratory dynamics," Entropy **17**, 277–303 (2015).
[48]W. H. Cooke, J. B. Hoag, A. A. Crossman, T. A. Kuusela, K. U. Tahvanainen, and D. L. Eckberg, "Human responses to upright tilt: a window on central autonomic integration," The Journal of physiology **517**, 617–628 (1999).
[49]T. J. Mullen, M. L. Appel, R. Mukkamala, J. M. Mathias, and R. J. Cohen, "System identification of closed-loop cardiovascular control: effects of posture and autonomic blockade," American Journal of Physiology-Heart and Circulatory Physiology **272**, H448–H461 (1997).
[50]R. Zhang, J. H. Zuckerman, C. A. Giller, and B. D. Levine, "Transfer function analysis of dynamic cerebral autoregulation in humans," American Journal of Physiology-Heart and Circulatory Physiology **274**, H233–H241 (1998).
[51]O. Paulson, S. Strandgaard, and L. Edvinsson, "Cerebral autoregulation." Cerebrovascular and brain metabolism reviews **2**, 161–192 (1990).
[52]L. Barnett, A. B. Barrett, and A. K. Seth, "Granger causality and transfer entropy are equivalent for gaussian variables," Physical review letters **103**, 238701 (2009).
[53]L. Barnett and A. K. Seth, "The mvgc multivariate granger causality toolbox: a new approach to granger-causal inference," Journal of neuroscience methods **223**, 50–68 (2014).
[54]L. Barnett and A. K. Seth, "Granger causality for state-space models," Physical Review E **91**, 040101 (2015).
[55]Y. Antonacci, L. Minati, D. Nuzzi, G. Mijatovic, R. Pernice, D. Marinazzo, S. Stramaglia, and L. Faes, "Measuring high-order interactions in rhythmic processes through multivariate spectral information decomposition," IEEE Access **9**, 149486–149505 (2021).

[56]A. Kraskov, H. Stögbauer, and P. Grassberger, "Estimating mutual information," Physical review E **69**, 066138 (2004).
[57]I. Vlachos and D. Kugiumtzis, "Nonuniform state-space reconstruction and coupling detection," Physical Review E **82**, 016207 (2010).
[58]L. Faes, G. Nollo, and A. Porta, "Non-uniform multivariate embedding to assess the information transfer in cardiovascular and cardiorespiratory variability series," Computers in biology and medicine **42**, 290–297 (2012).
[59]M. Papapetrou, E. Siggiridou, and D. Kugiumtzis, "Adaptation of partial mutual information from mixed embedding to discrete-valued time series," Entropy **24** (2022).
[60]A. Porta, V. Bari, A. Marchi, B. De Maria, P. Castiglioni, M. Di Rienzo, S. Guzzetti, A. Cividjian, and L. Quintin, "Limits of permutation-based entropies in assessing complexity of short heart period variability," Physiological measurement **36**, 755 (2015).
[61]D. Cuesta-Frau, M. Varela-Entrecanales, A. Molina-Picó, and B. Vargas, "Patterns with equal values in permutation entropy: Do they really matter for biosignal classification?" Complexity **2018** (2018).
[62]C. Bian, C. Qin, Q. D. Ma, and Q. Shen, "Modified permutation-entropy analysis of heartbeat dynamics," Physical Review E **85**, 021906 (2012).
[63]D. Cuesta Frau, "Permutation entropy: Influence of amplitude information on time series classification performance," Mathematical Biosciences and Engineering **16**, 6842–6857 (2019).
[64]A. Myers and F. A. Khasawneh, "On the automatic parameter selection for permutation entropy," Chaos: An Interdisciplinary Journal of Nonlinear Science **30**, 033130 (2020).
[65]F. Battiston, G. Cencetti, I. Iacopini, V. Latora, M. Lucas, A. Patania, J.-G. Young, and G. Petri, "Networks beyond pairwise interactions: structure and dynamics," Physics Reports **874**, 1–92 (2020).

AIP Publishing

Chaos
An Interdisciplinary Journal
of Nonlinear Science

PLEASE CITE THIS ARTICLE AS DOI: 10.1063/5.0140641

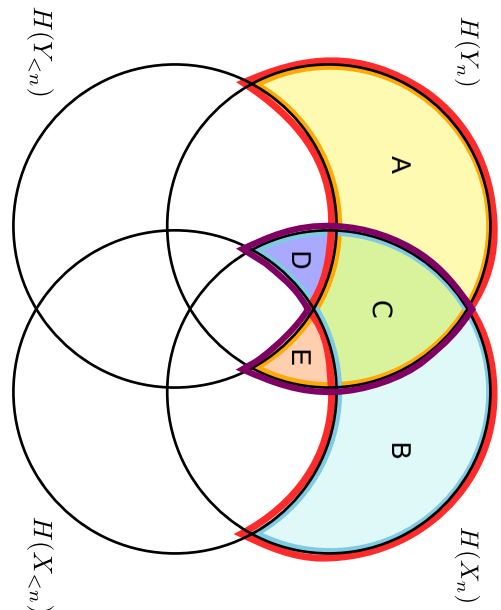

Chaos
An Interdisciplinary Journal
of Nonlinear Science

AIP Publishing

PLEASE CITE THIS ARTICLE AS DOI: 10.1063/5.0140641

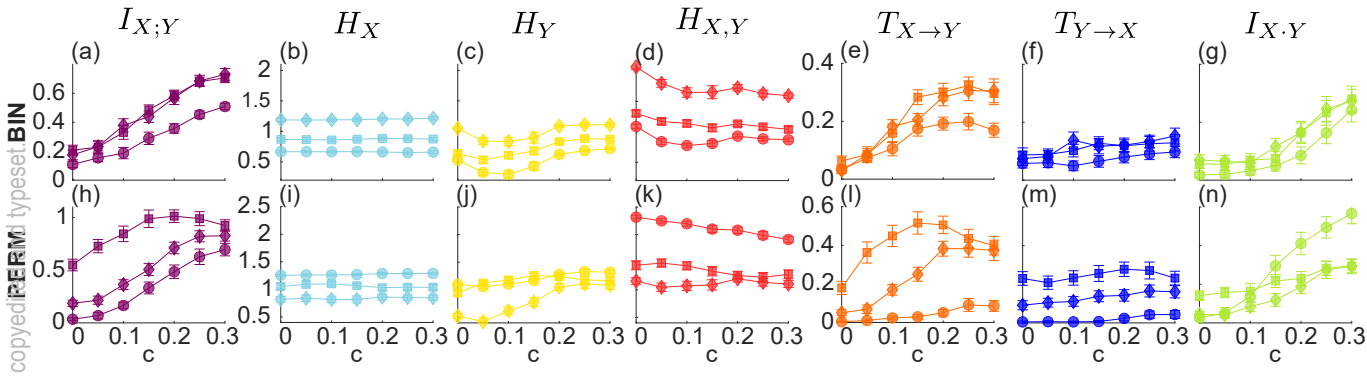

AIP Publishing

Chaos
An Interdisciplinary Journal
of Nonlinear Science

PLEASE CITE THIS ARTICLE AS DOI: 10.1063/5.0140641

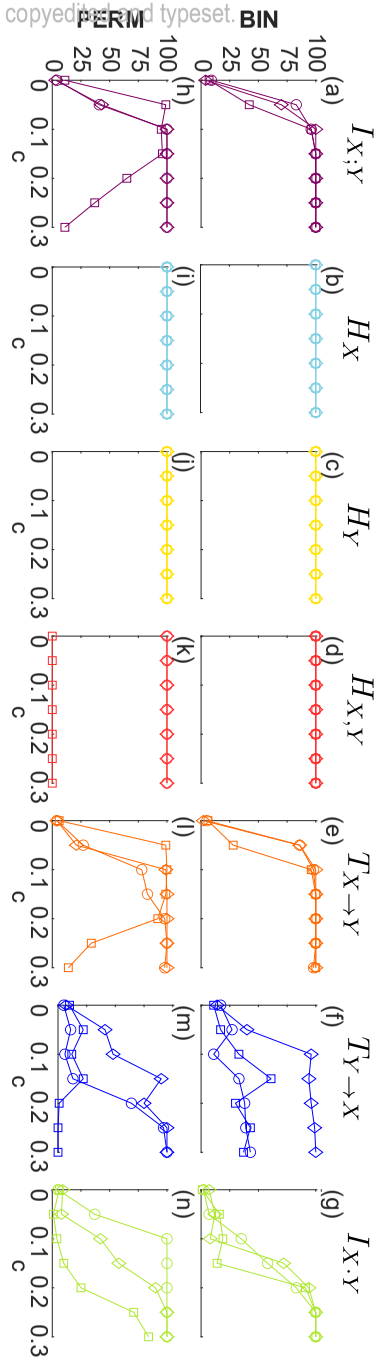

AIP Publishing

Chaos
An Interdisciplinary Journal
of Nonlinear Science

PLEASE CITE THIS ARTICLE AS DOI: 10.1063/5.0140641

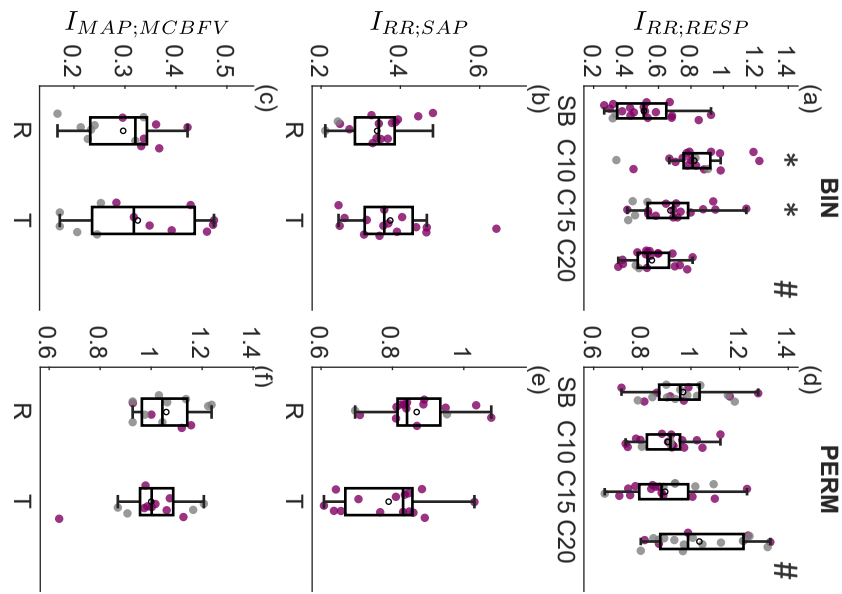

AIP Publishing

Chaos
An Interdisciplinary Journal
of Nonlinear Science

PLEASE CITE THIS ARTICLE AS DOI: 10.1063/5.0140641